



OPEN Enhancing mechanical properties of low plasticity soil through coal and silica fume stabilization

Muhammad Waleed^{1,2} & Fahad Alshawmar³✉

Low-plasticity soils, characterized by low plasticity and high sand content, present challenges in engineering projects due to their inadequate strength and stability. This study evaluates the comparative effects of coal waste and silica fume as stabilizers to improve the mechanical properties of silty soils. Key parameters such as liquid limit (LL), plastic limit (PL), plasticity index (PI), maximum dry density (MDD), unconfined compressive strength (UCS), and shear strength were assessed through laboratory experiments with varying stabilizer proportions (3–12%). Results showed that silica fume increased the LL of Tarnol soil by 36% and reduced its PI, while coal waste improved the LL of Chaklala soil by 48%, also reducing its PI. Both stabilizers decreased MDD and increased optimum moisture content (OMC). Notably, UCS increased by 77% in Tarnol soil with 12% silica fume and by 83% in Chaklala soil with 12% coal waste after 28 days of curing. Coal waste improved the cohesion of Chaklala soil by a factor of 1.29 and its internal friction angle by 1.04, while silica fume enhanced Tarnol soil cohesion by 1.35 and its internal friction angle by 1.032. These findings demonstrate the potential of coal waste and silica fume as cost-effective, sustainable stabilizers for improving the geotechnical performance of low-plasticity soils. The study contributes valuable insights into using industrial by-products for soil stabilization, offering practical applications for enhancing soil strength and stability in construction and infrastructure projects.

Keywords Silica fume, Coal waste, Low plastic soil, Soil, Stabilization, Sustainability

Soil types serve as crucial foundation materials in civil engineering projects. Structures such as roads, bridges, buildings, and dams ultimately transfer their loads to the foundation soils¹. Soil stabilization is a procedure performed by various researchers to enhance the strength, stability, and other engineering and physical properties of a specific soil mass, often utilizing waste materials to promote sustainability^{2–10}. Enhancing the shear strength of soil, increasing its load-bearing capacity, and mitigating shrink-swell behavior through stabilization techniques not only improve engineering performance but also reduce the risk of unfavorable engineering behavior¹¹. Low-plasticity silt soil is significant in geotechnical engineering applications due to its distinct characteristics and behavior. According to the Unified Soil Classification System (USCS), this type of soil has a low plasticity index (PI) and is categorized as ML soil¹². It typically has a low moisture content and consists of fine-grained particles with sizes ranging from 0.002 mm to 0.075 mm. Silt soils are highly sensitive to moisture, and the degree of densification achieved during compaction significantly impacts their stability¹³. Silty soils are often hydrophobic and challenging to prepare for compaction at a reasonable cost when it comes to moisture conditions¹⁴. However, low-plasticity silt soil can be vulnerable to problems such as liquefaction during earthquakes and settlement due to fluctuations in moisture content^{15,16}. When building structures and foundations in areas with low-plasticity silt soil, engineers must carefully account for the characteristics and behavior of this soil type. Low-plasticity silt soil is notable in geotechnical engineering applications, presenting both benefits and challenges due to its unique features and behavior¹⁷. Some researchers have utilized waste materials to enhance the strength properties of low plastic soils. Asgari, et al.¹⁸ combined cement with lime and observed improvements in the bearing capacity and durability of the soil. Another study Turkane and Chouksey¹⁹ used fly ash in low plastic soil and observed the maximum increase in soil strength by incorporating 25% ash. The study by Muntohar, et al.²⁰ utilized rice husk ash combined with waste plastic fiber in low plastic soil and observed an increase in the bearing capacity and shear strength of the soil. Further research is necessary to better understand this soil type and effectively mitigate associated risks. One environmental concern is the

¹Civil Engineering Department, National University of Modern Languages, Rawalpindi 44000, Pakistan. ²NUST Institute of Civil Engineering, National University of Sciences and Technology (NUST), Islamabad 44000, Pakistan.

³Department of Civil Engineering, College of Engineering, Qassim University, Buraydah 51452, Saudi Arabia. ✉email: shomr@qu.edu.sa

potential for heavy metal leakage from coal waste into subsurface resources due to its hazardous heavy metal content²¹. Researchers are increasingly exploring coal waste as an alternative for soil stabilization due to its low cost, availability, and potential for effective stabilization^{22–27}. By 2030, it is anticipated that coal, which is primarily composed of carbon but also contains varying proportions of hydrogen, sulfur, oxygen, and nitrogen, will supply approximately 50% of the world's energy needs^{25,28}. Even though coal waste contains hazardous chemicals like lead, mercury, and arsenic, with proper management, it can be a sustainable and efficient way to stabilize soil. It could decrease soil erosion and increase soil strength while providing a more affordable option to conventional stabilizers²⁹. But it's important to pay close attention to the possible environmental hazards, like soil and groundwater poisoning from heavy metals. The adverse effects on the environment can be reduced by putting treatment procedures in place to lessen these metals' mobility and by tracking soil changes over time³⁰. Coal waste can provide sustainable soil stabilization without affecting the well-being of the environment if the right safety measures are taken and more study is done on better management techniques.

Silica fume and coal improve soil quality by reducing the plasticity index (PI) and optimum moisture content (OMC), which in turn enhances its engineering properties, such as durability, unconfined compressive strength (UCS), and hydraulic conductivity. Various additives, including cement, lime, enzymes, industrial waste, fly ash, bagasse ash, nanomaterials, and rice husk, have been used to alter the engineering properties of problematic soils^{31–38}.

Mansouri et al.³⁹ studied coal waste as a clayey soil stabilizer in road construction, testing 3–12% coal waste and 4–6% lime. Results showed reduced liquid limits, increased maximum dry density (MDD), and higher optimum moisture content (OMC), enhancing soil strength. Afrakoti et al.²⁶ investigated coal waste's impact on soil mechanics, finding that adding 5% coal waste with 6% cement improved properties. However, replacing cement with coal waste reduced mechanical strength, especially with 3% cement. Modarres and Nosoudy^{40,41} used coal waste and lime for soil stabilization of clayey soil, noting a reduced liquid limit (LL), unchanged plastic limit (PL), increased maximum dry density (MDD), and decreased optimum moisture content (OMC). Both additives improved the California Bearing Ratio (CBR) and compressive strength, with lime activating the coal waste. Turkoz et al.⁴² examined the effect of silica fume on dispersive soil, finding reduced liquid limit (LL) and overall plasticity, with minimal change in the plastic limit (PL). The addition increased optimum moisture content (OMC) and decreased maximum dry density (MDD) due to silica fume's low density. The initial shear modulus improved with silica fume. Al-Obaidi, et al.⁴³ investigated silica fume and nanosilica in improving the collapsibility and shear strength of highly gypseous soil. Both additives enhanced soil properties, especially under saturated conditions, with silica fume increasing cohesiveness by 140–310% in dry soil and 20–40% in saturated soil. However, silica fume's water demand could have adverse effects. AL-Soundany⁴⁴ studied silica fume in expansive soil, finding that increased bentonite content significantly raised the liquid limit (LL), while silica fume reduced it. Higher bentonite content also increased the plastic limit (PL) and plasticity index (PI), but silica fume decreased PI by binding clay particles. Specific gravity decreased with bentonite but increased with silica fume. The optimum moisture content (OMC) rose with bentonite, while maximum dry density (MDD) decreased as bentonite content increased.

Previous research has primarily focused on examining the influence of silica fume and coal on various soil types mostly on the clayey soil. However, there is a significant gap in the literature regarding the assessment of silica fume and coal's impact on stabilizing low-plasticity silt soil because they naturally exhibit poor strength, low cohesion, and high susceptibility to erosion and settlement under load. Stabilizing these soils with silica fume and coal ash enhances their engineering properties by reducing plasticity, increasing strength, and improving compaction and durability. This study aims to address this gap by doing a comparative analysis of silica fume and coal to specifically enhance the properties of low-plasticity soil through the use of waste materials.

Materials used

Soil

The soil samples were collected from the Tarnol and Chaklala regions of Pakistan at a depth ranging from 0.5 to 1 m, as shown in Fig. 1. The collected samples were dried in an oven at 110 °C. According to the Unified Soil Classification System (USCS), the soils are categorized as low-plasticity silt soils (ML), and based on the American Association of State Highway and Transportation Officials (AASHTO) classification, they are classified as A-4. The Fig. 2 shows the grain size distribution curves for the two soil types. Table 1 provides a comprehensive overview of the physical properties of both Chaklala and Tarnol soils. The chemical composition of the Chaklala and Tarnol soils is detailed in Table 2, which specifies the quantities of various elements and compounds present in each soil sample. According to Table 2, both soils have a high content of SiO₂, with Chaklala soil containing 41.54% and Tarnol soil containing 56.54% SiO₂. Both soils may have different physical and geotechnical characteristics, such as variations in particle size distribution, mineral composition, and natural moisture content, even if they are classified as the same. These differences make it possible to examine the responses of various low-plasticity silts to stabilization techniques in a more comprehensive manner. By evaluating two different soils in the same category, the study can offer a more thorough and general understanding of how well coal ash and silica fume enhance the mechanical qualities of low-plasticity soils, guaranteeing that the results are applicable to a larger range of comparable soil types in practical engineering applications.

Coal

Coal (C) is a combustible organic substance widely used as a primary ingredient in various industries⁴⁵. It resembles charcoal in appearance and is produced by burning organic materials such as wood chips, leaves, or dead plants. Coal typically consists of about 70% carbon, with the remaining 30% comprising nitrogen, hydrogen, and oxygen⁴⁶. The physical and chemical properties of coal can influence soil structure and consistency. Coal has

Material	Oxide content (%)											
	CaO	SiO ₂	Al ₂ O ₃	SO ₃	Fe ₂ O ₄	TiO ₂	MgO	P ₂ O ₅	MnO	K ₂ O	ZnO	Others
Chaklala soil	12.43	41.54	21.43	0.67	15.43	2.65	2.23	0.95	-	1.76	-	0.91
Tarnol soil	1.75	56.54	19.76	1.54	10.56	1.43	0.65	-	1.65	2.90	2.50	0.72

Table 2. Chemical composition of Chaklala and Tarnol soils.

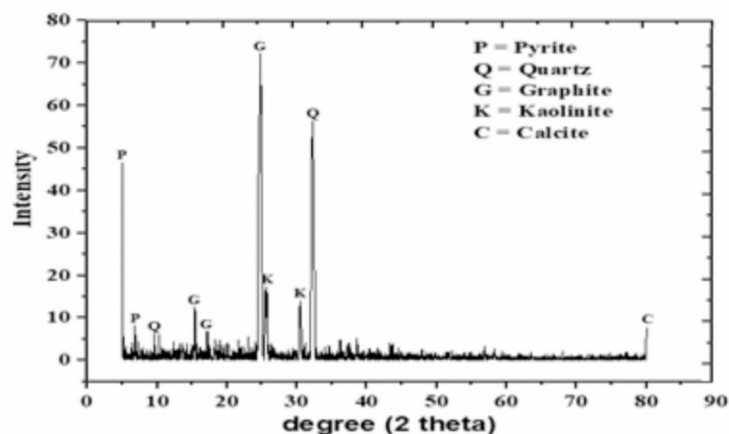


Fig. 3. X-ray diffractograms of the coal considered in this study for the identification of various peaks.

Mineralogical composition								
Material	Mineral content (%)							
	Graphite	Quartz	Kaolinite	Pyrite	Calcite	Others		
Coal	91.3	3.2	2.1	1.7	1.4	0.3		
Chemical composition								
Material	Oxide content (%)							
	CaO	SiO ₂	Al ₂ O ₃	Fe ₂ O ₄	TiO ₂	MgO	K ₂ O	Others
Coal	2.43	60.76	22.43	9.65	1.15	1.54	1.15	0.89

Table 3. Mineralogical and chemical composition of coal.

also been utilized to aid in the reclamation of degraded soils. In this study, coal waste was collected from the local market, and the X-ray diffractogram of the coal is shown in Fig. 3.

The chemical and mineralogical compositions of coal, as determined by X-ray fluorescence (XRF) spectrometry, are displayed in Table 3. According to the table, coal has the highest mineral content of graphite at approximately 91.3%, while its chemical composition shows the highest SiO₂ content at about 60.76%

Silica fumes

Silica fume (SF), also known as microsilica, is a by-product of silicon and ferrosilicon alloy production⁴⁷. It is a highly reactive pozzolan that reacts with calcium hydroxide in the presence of water to form additional cementitious compounds. Silica fume is commonly used as an additive in concrete to enhance its strength and durability^{48,49}. Due to its chemical and physical properties, it is a very reactive pozzolan^{50,51}. While primarily used in concrete, silica fume can also be beneficial for improving silty soil conditions. Silica fume can be mixed with soil to enhance its compaction and stability. Incorporating silica fume improves soil density and reduces compressibility, making the soil more resistant to settlement and deformation. Silty soils often have low strength and are prone to shear failure; the introduction of silica fume significantly increases soil strength, thereby improving its load-bearing capacity⁵². Silica fume acts as a filler and binder, creating a stronger matrix within the soil. In this study, silica fume was collected from the local market, and the X-ray diffractogram of the silica fume is shown in Fig. 4.

Table 4 displays the mineralogical and chemical composition of silica fume as measured by X-ray fluorescence (XRF) spectroscopy. The mineralogical composition indicates that silica fume contains 87.6% quartz, the highest amount among its components. Chemically, silica fume is predominantly composed of SiO₂, constituting 94.54% of its content.

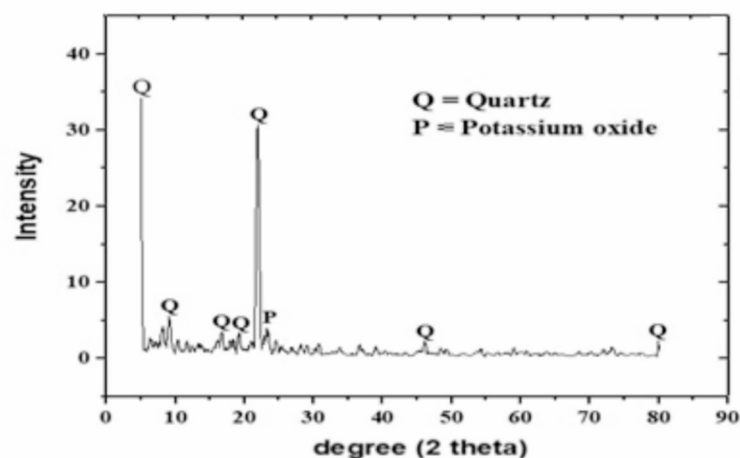


Fig. 4. X-ray diffractograms of the silica fume considered in this study for identification of various peaks.

Mineralogical composition											
Material	Mineral content (%)										
	Quartz	Potassium oxide	Others								
Silica fume	87.6	11.5	0.9								
Chemical composition											
Material	Oxide content (%)										
	CaO	SiO ₂	Al ₂ O ₃	SO ₃	Fe ₂ O ₄	TiO ₂	MgO	P ₂ O ₅	MnO	K ₂ O	Others
Silica fume	1.21	94.54	0.54	0.21	0.65	0.02	0.82	1.15	0.39	0.03	0.44

Table 4. Mineralogical and chemical composition of silica fume.

Methodology

Liquid limit test

The test was conducted following ASTM D432-66 guidelines, as shown in Fig. 5. The liquid limit (LL) test determines the water content at which soil transitions from a plastic to a liquid state. A natural soil sample with a specific water content is placed in a brass cup, and a standard cone is dropped into the soil to measure the number of blows required to close a 12.7 mm groove, determining the LL. For the Tarnol soil sample, silica fume was added in varying proportions (3%, 6%, 9%, and 12%), replacing an equivalent percentage of soil. For the Chaklala soil sample, coal was substituted in the same proportions. Both modified and natural soil samples were tested using the same procedure, recording the number of blows and the weights of dry and moist samples.

Plastic limit test

The experiment followed ASTM D698-70 guidelines, as shown in Fig. 5. The plastic limit (PL) test measures the water content at which soil transitions from a plastic to a semi-solid state by rolling a 3 mm thread of soil until it crumbles. For the Tarnol soil sample, silica fume was added in increments of 3%, 6%, 9%, and 12%, replacing corresponding soil percentages, and tested similarly to natural soil. For the Chaklala soil sample, coal was added in the same proportions and tested using the same procedure.

Standard proctor test

The test followed ASTM D698-12 guidelines to evaluate soil compaction characteristics, specifically maximum dry density (MDD) and optimum moisture content (OMC). The Standard Proctor Test involved compacting soil into a mold using a 2.5 kg hammer with 25 blows per layer in three layers, increasing water content by 3% per trial, as shown in Fig. 5. For the Tarnol soil sample, silica fume was added in increments of 3%, 6%, 9%, and 12%, replacing a percentage of the soil, and tested under the same conditions as the natural soil. Similarly, the Chaklala soil sample used coal as an additive in the same proportions, with all weight data recorded in the datasheet.

Unconfined compressive strength (UCS)

The unconfined compressive strength (UCS) test of the soil was conducted following the guidelines outlined in the D2166⁵³, as shown in Fig. 5. This test measures the compressive strength of soil samples without lateral confinement, providing a quick assessment of soil stability. A strain rate of 1 mm/min was applied to evaluate

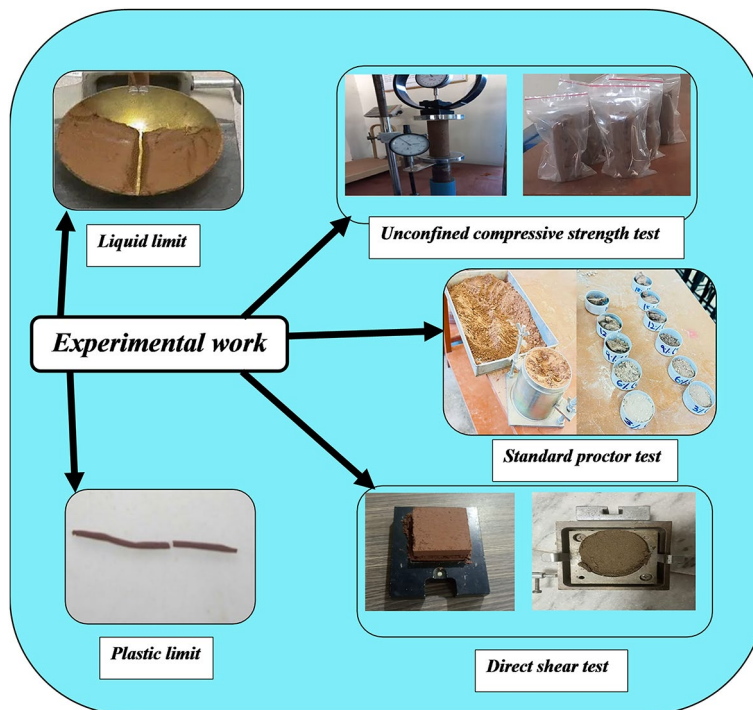


Fig. 5. Soil mechanical tests performed in the study.

strength differences between coal-treated and silica-fume-treated soils. Specimens were prepared with 3%, 6%, 9%, and 12% of each additive, molded into cylindrical shapes (height-to-diameter ratio of 2:1), sealed in plastic bags to retain moisture, and cured at 20 °C for 7, 14, 21, and 28 days. After curing, specimens were subjected to axial loading until failure, and the peak load was recorded to determine UCS values.

Direct shear test

The specimens for the direct shear test were prepared using samples with dimensions of 60 mm x 60 mm x 30 mm, as shown in Fig. 5. The direct shear test was conducted in accordance with the guidelines outlined in the ASTM D3080 standard⁵⁴. Soil samples were prepared with 3%, 6%, 9%, and 12% silica fume and coal, then placed in a shear box, allowing horizontal movement of the upper half relative to the lower half. A vertical load maintained normal pressure as the horizontal shear force increased until failure. The direct shear test determined critical parameters like the angle of internal friction and cohesion, essential for understanding shear strength. The results, as shown in Fig. 5, highlight how varying concentrations of silica fume and coal enhance soil resistance to shear stress, providing insights into improved soil stability.

SEM test

The soil samples underwent Scanning Electron Microscopy (SEM) testing in compliance with ASTM E2809 guidelines for microstructural examination. The samples included both natural soil and soil treated with 12% coal and 12% silica fume. Initially, in order to ensure total moisture evaporation, the samples were kept in an oven set at 35 °C for 24 h. In order to avoid any thermal effects that can change the structure of the soil, this moderate temperature for drying was selected. To prevent any moisture absorption from the air, the samples were taken out of the oven and cooled to room temperature in a desiccator. By ensuring that the soil samples were stable and dry prior to SEM examination, this technique reduced the possibility of artifacts that can affect the interpretation of the microstructural features. This information is crucial for understanding how these additives enhance soil properties by improving particle interlocking and reducing void spaces, which can contribute to increased strength and stability.

Results and discussion

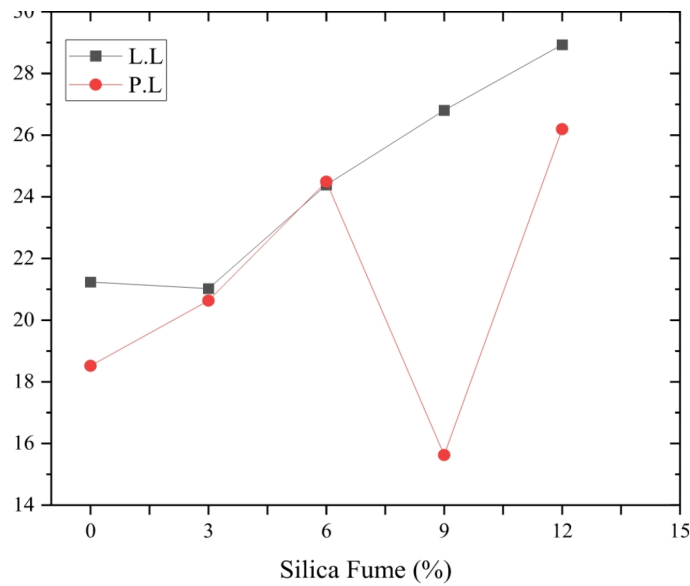
Atterberg's limits

Chaklala soil exhibits a liquid limit (LL) of 17.29%, a plastic limit (PL) of 15%, and a plasticity index (PI) of 2.29%. Conversely, Tarnol soil shows an LL of 21.23%, a PL of 18.51%, and a PI of 2.71%. These results indicate that both soils possess low plasticity and a limited capacity for shrinkage and swelling, suggesting they are unlikely to experience significant volume changes, as evidenced by their low plasticity indices.

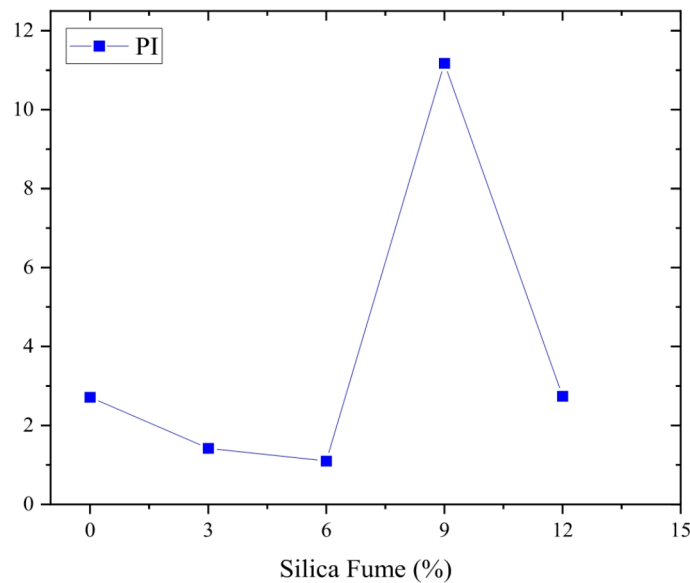
Atterberg's limits for Tarnol soil amended with silica fume

In the case of Tarnol soil amended with silica fume (SF), both the LL and PI initially decrease before increasing as the SF content rises. When 3% SF is added, the LL of the soil decreases slightly by 1%. However, as the SF

content increases to 12%, the LL rises significantly by up to 36%, indicating an overall increase in LL with higher SF content, as depicted in Fig. 6(a). Silica fume has an extremely high surface area due to its fine particle size, increases the soil's overall surface area when incorporated in soil, enhancing its water-holding capacity and leading to a higher LL. Additionally, the SF dispersed the clay particles, increasing interparticle spacing and enabling the soil matrix to retain more water, leading to a rise in LL. This increase is also attributed to the reduction in alumina content due to the excessive addition of SF, corroborating findings from prior research⁵⁵.



(a)



(b)

Fig. 6. Atterberg's limits for Tarnol soil amended with silica fume: **(a)** liquid and plastic limits; **(b)** plasticity index.

The PL demonstrates a similar trend, initially increasing and then decreasing, reaching a maximum of 9% SF content before rising again, as illustrated in Fig. 6(a). At first, when the silica fume level rises to 6%, it fills in gaps and strengthens the bond, increasing PL by increasing plasticity and water retention. At 9%, silica fume and clay minerals undergo a more intense pozzolanic reaction, strengthening the linkages and decreasing the soil's capacity to hold water, which lowers PL. PL rises at 12%, though, as the ongoing pozzolanic reaction further stabilizes the soil structure and creates a more compact and well-bound matrix, which improves the soil's capacity to hold onto moisture. This pattern aligns with trends observed in previous studies, such as those reported by⁵⁶.

The plasticity index (PI) reaches its maximum value at 9% SF addition, indicating that the soil experiences the most significant increase in plasticity at this specific level of silica fume incorporation, as illustrated in Fig. 6(b). However, beyond 9%, particularly at 12% SF addition, the plasticity of the soil decreases. At 3–6% silica fume content, PI decreases as flocculation and agglomeration of clay particles reduce plasticity. The fine silica particles adsorb onto the clay surface, limiting water retention and reducing the gap between LL and PL. PI rises at 9% silica fume content because an excess of fine silica particles improve water retention, slow down pozzolanic processes, and marginally increase plasticity. The gap between LL and PL is significantly increased as a result. Stronger pozzolanic reactions at 12% silica fume cause PI to drop once more, enhancing cementation and particle aggregation while decreasing soil plasticity and stabilizing the soil. This reduction in PI mainly attributed to the enhanced pozzolanic reaction between silica fume and aluminous materials in the soil, as indicated by the findings⁵⁶.

The fundamental mechanism behind the changes in physical properties induced by silica fume, which ultimately lead to variations in mechanical properties, is primarily attributed to particle interaction, pozzolanic reactions, and microstructural modification. As silica fume content increases, pozzolanic reactions occur, forming cementitious compounds that bond soil particles together. Higher LL and PL values show that the soil can hold onto moisture better while retaining its structural integrity, which improves the soil structure, leading to increased shear strength, soil's workability and compaction properties. By reducing excessive volume variations based on by moisture fluctuations, the drop in PI indicates decreased soil flexibility and improves the soil's resilience to swelling and shrinkage. This enhancement is very helpful for improving shear strength, decreasing settlement problems, and stabilizing soils. Furthermore, by strengthening interparticle interaction, the fine silica fume particles aid in altering the soil matrix and creating a more resilient and stable soil structure.

Atterberg's limits for Chaklala soil amended with coal

The impact of coal addition on the liquid limit (LL) and plastic limit (PL) of Chaklala soil is depicted in Fig. 7(a). The LL and plasticity index (PI) of the soil initially increase with certain coal content, then decrease at intermediate coal percentages, and finally increase again as the coal content continues to rise. Specifically, the LL of the soil increases by 34% with a 3% coal addition, reaching a 48% increase at 12% coal content. This trend is also observed for the PL, although a decrease occurs at 6% coal content, likely due to the optimal range for achieving maximum plasticity.

Overall, both the PL and LL tend to increase with higher coal content in the soil. The increase in LL can be attributed to changes in soil behavior resulting from the altered particle size distribution. The fine particles introduced by coal enhance plasticity and LL. Additionally, the organic richness of coal acts as a binding agent, improving soil plasticity and water retention, thereby further increasing the LL.

The plasticity index (PI) of the soil increased with the addition of coal up to 6%, reaching a value 3.3 times higher than that of the natural soil, as shown in Fig. 7(b). However, at 9% coal content, the PI decreased. This fluctuation in PI can be attributed to the water absorption and retention capabilities of coal. Coal's ability to absorb and retain water significantly alters the consistency limits of the soil. These findings are consistent with previous research studies^{57,58}.

Compaction characteristics

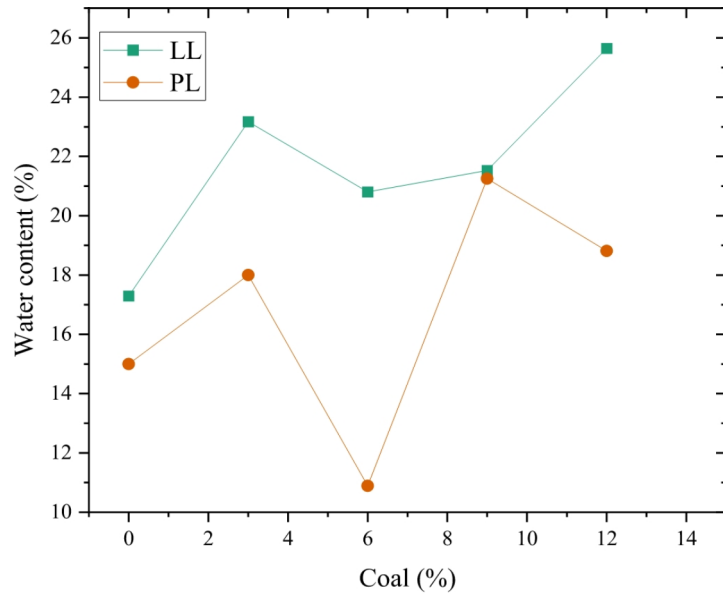
Compaction characteristics of Tarnol soil modified with silica fume

Figure 8 illustrates that the maximum dry density (MDD) of natural Tarnol soil was 24.568 kN/m³ at an optimum moisture content (OMC) of 11.85%. The addition of silica fume (SF) resulted in a decrease in MDD and an increase in OMC, as depicted in Fig. 8. Specifically, with the incorporation of 3% SF, the MDD decreased to 18.68 kN/m³, and the OMC increased to 13.04%. The reduction in MDD is attributed to the fine nature of silica fume, which fills the voids between soil particles, leading to a denser particle arrangement. This densification can lower the MDD and may reduce the cohesive forces among soil particles, thereby disrupting the natural soil structure. As a result, the soil's compaction potential diminishes, further decreasing the MDD⁴⁴.

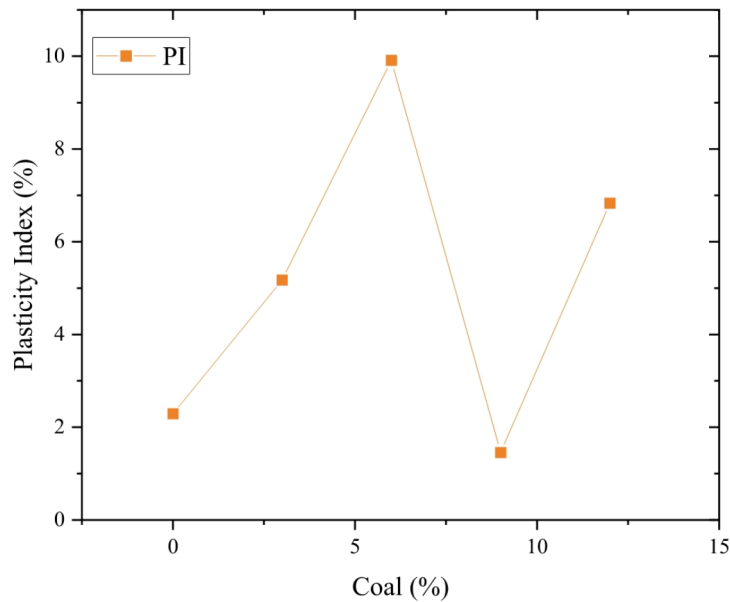
The MDD decreased as the silica fume percentage increased from 0 to 12%, as shown in Fig. 9. This decrease is mostly caused by the lower specific gravity of silica fume than that of soil particles, which makes the soil-additive mixture lighter. Moreover, the fine texture of silica fume creates more void spaces in the mixture, which further lowers the density. Similarly, when the amount of silica fume increased, the OMC tended to decrease, as shown in Fig. 9. This is explained by the high water absorption capacity of silica fume, which slows the hydration process and lowers the amount of water available to achieve the optimum density.

Compaction characteristics of Chaklala soil modified with coal

Figure 10 shows that Chaklala soil exhibited a maximum dry density (MDD) of 18.41 kN/m³ at an optimum moisture content (OMC) of 13.53%. The MDD of the soil was achieved after the addition of 3% coal, which resulted in an MDD of 17.83 kN/m³ and an OMC of 14.73%, as illustrated in Fig. 10. The observed decrease in MDD with the addition of coal, along with the increase in moisture content, can be attributed to the effects of coal on soil structure. The introduction of coal may induce particle rearrangement within the soil, leading to a



(a)



(b)

Fig. 7. Atterberg's limits for Chaklala soil amended with coal: **(a)** liquid and plastic limits; **(b)** plasticity index.

less compacted structure and thus reducing the MDD. Furthermore, coal's water-retaining properties contribute to an increased water content within the soil matrix, resulting in a higher OMC.

The fact that MDD varies indicates that the presence of coal has a significant impact on soil compatibility, as shown in Fig. 11. Higher coal percentages cause a decrease in MDD, which may indicate that too much coal causes voids and lowers soil density. The dual function of coal particles as structural modifiers and water-absorbing agents is reflected in the OMC behavior. Figure 11 shows that the OMC increases significantly at 12%, suggesting that a higher coal content requires more water because of the coal's capacity to absorb water and the

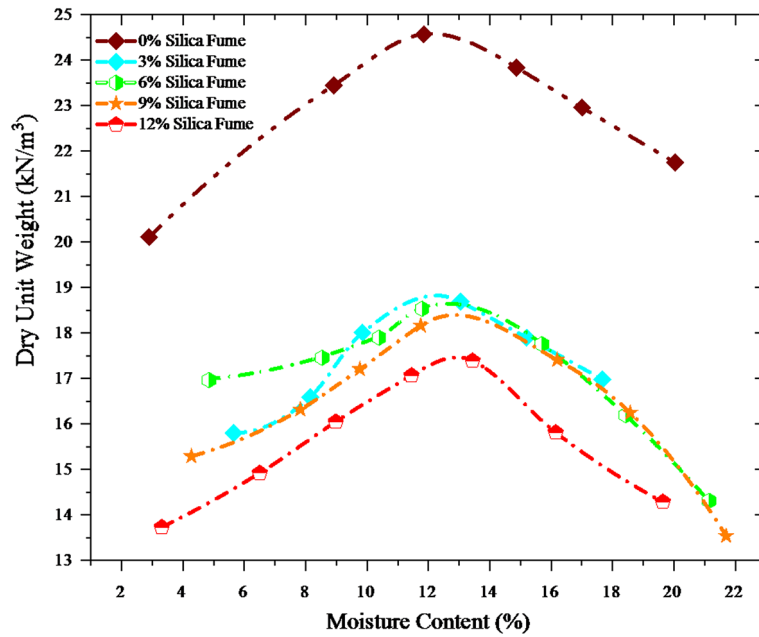


Fig. 8. Moisture density relationship curves obtained from various levels of silica fume (SF) in soil mixtures.

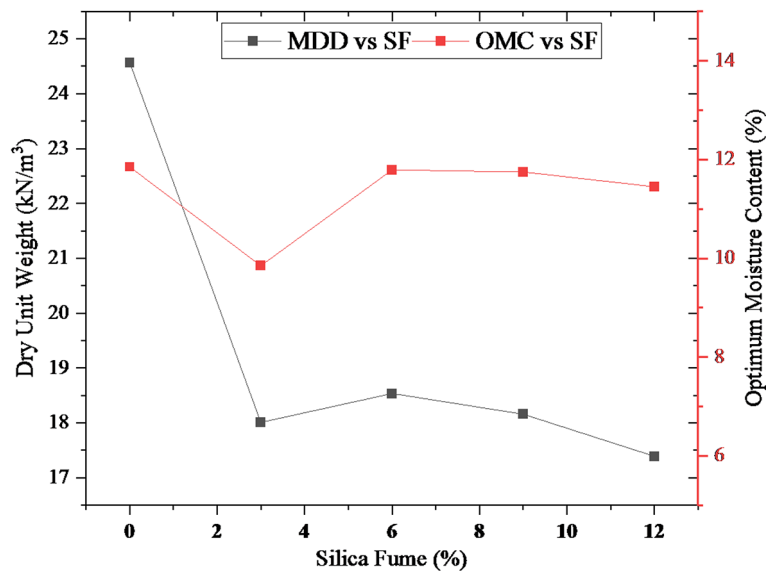


Fig. 9. Variation of optimum moisture content (OMC) and maximum dry density (MDD) as a function of silica fume (SF) content.

larger void spaces that need moisture to be compacted. This suggests that to obtain the ultimate results during stabilization attempts, the water content must be carefully balanced.

Curing effects

Effect of curing on the Tarnol soil amended with silica fume

Figure 12 illustrates the effect of curing on the unconfined compressive strength (UCS) of soil stabilized with silica fume (SF). The data for curing periods of 7, 14, 21, and 28 days are presented alongside the corresponding SF percentages. The results demonstrate a notable enhancement in UCS with SF treatment. The UCS of the natural soil was measured at 60.96 kPa and remained consistent throughout the curing period. The highest UCS, reaching 108.1 kPa, was achieved with a sample containing 12% SF after 28 days of curing, as shown in Fig. 12. The increase in UCS with higher SF percentages is evident across all curing intervals (7, 14, 21, and 28 days). However, it is observed that the rate of increase in UCS diminishes after 14 days compared to the increases seen at 7 and 14 days. The results indicate that an increase in curing time does not significantly contribute to the UCS

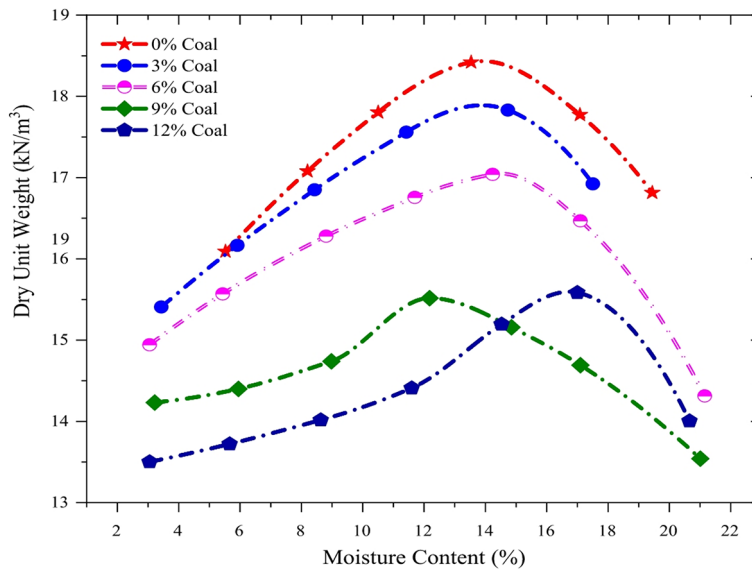


Fig. 10. Moisture density relationship curves obtained from various levels of coal (C) in soil mixtures.

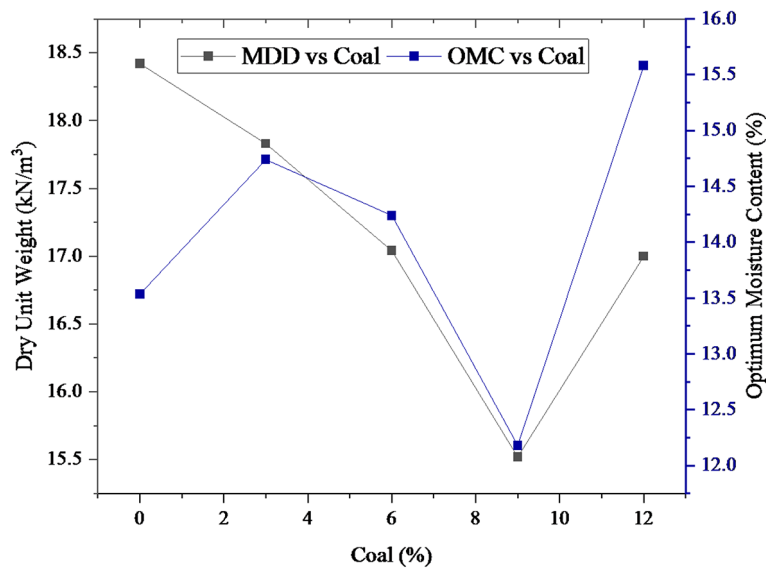


Fig. 11. Variation of optimum moisture content (OMC) and maximum dry density (MDD) as function of coal (C) content.

value beyond 14 days. However, an increase in the percentage of silica fume and coal ash leads to a notable rise in UCS. Nonetheless, extended curing time still positively affects UCS, as the calcium silicate hydrate (C-S-H) gels formed during pozzolanic reactions bind soil particles together, enhancing cohesiveness and reducing porosity. As the curing process continues, more C-S-H gels are produced, further strengthening the soil matrix. These observations align with similar findings reported in the study by⁵⁹. SF enhances the bonding and cohesion among soil particles due to its pozzolanic properties^{44,60}. Additionally, SF exhibits adhesive characteristics, particularly when subjected to curing⁶¹. This adhesive nature effectively binds soil particles together, thereby increasing the soil’s resistance to deformation and enhancing its compressive strength. Furthermore, SF has been found to reduce the plasticity of soil, which contributes to UCS⁴². By reducing soil plasticity, SF helps mitigate the detrimental effects of curing on soil properties, such as swelling and shrinkage, ultimately leading to improved strength characteristics.

Effect of curing on the Chaklala soil amended with coal

Figure 13 illustrates the impact of the curing period on the unconfined compressive strength (UCS) of soil stabilized with coal. The results for curing periods of 7, 14, 21, and 28 days are presented alongside the corresponding coal percentages. The maximum UCS value of 83.2 kPa was achieved with a sample containing 12% coal after a 28-

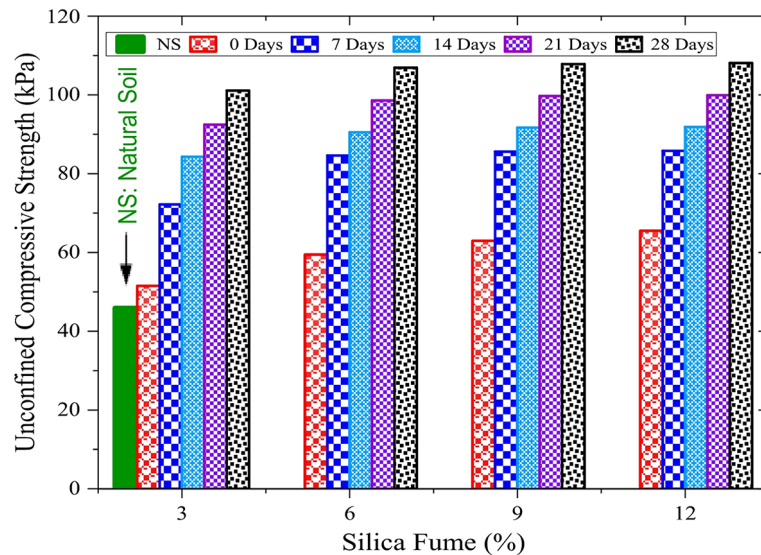


Fig. 12. Unconfined compressive strength of silica fume stabilized soil at 7, 14, 21 and 28 days of curing.

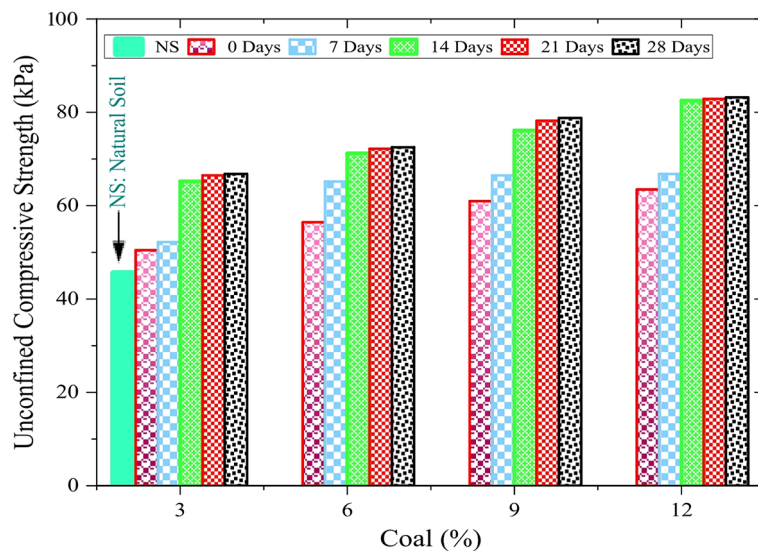


Fig. 13. Unconfined compressive strength of coal stabilized soil at 7, 14, 21 and 28 days of curing.

day curing period, as shown in Fig. 13. It was observed that UCS values for natural soil (without coal) remained constant across all curing periods. As the percentage of coal in the soil increases, the UCS values for the 7, 14, 21, and 28-day curing periods also increase. However, the rate of increase in UCS diminishes after 14 days compared to the increases observed at 7 and 14 days. This suggests that extending the curing period does not significantly enhance UCS, whereas higher coal content continues to improve compressive strength relative to the 7 and 14-day curing periods. Coal's porous structure contributes to increased soil porosity, which enhances drainage and reduces susceptibility to water-induced degradation during curing. This improvement in drainage and reduced water-related issues ultimately leads to enhanced compressive strength of the soil³⁹. Similar to silica fume, coal may reduce the plasticity properties of soil⁴⁰. This reduction in plasticity helps mitigate the adverse effects of curing, such as swelling and shrinkage, thereby enhancing the soil's strength characteristics. Additionally, research suggests that coal improves the mechanical properties of soil by enhancing the binding between soil particles²⁶. As coal content increases, the binding within the soil structure becomes more pronounced, leading to greater resistance to deformation and higher compressive strength.

Pozzolanic reactions between the stabilizing chemicals (such as silica fume or coal ash) and the minerals in the soil, particularly calcium compounds, are the technique causing the increase in unconfined compressive strength (UCS) with curing time. The calcium silicate hydrate (C-S-H) gels created by these reactions bind soil particles together, increasing cohesiveness and decreasing porosity. More C-S-H gels are created as the curing

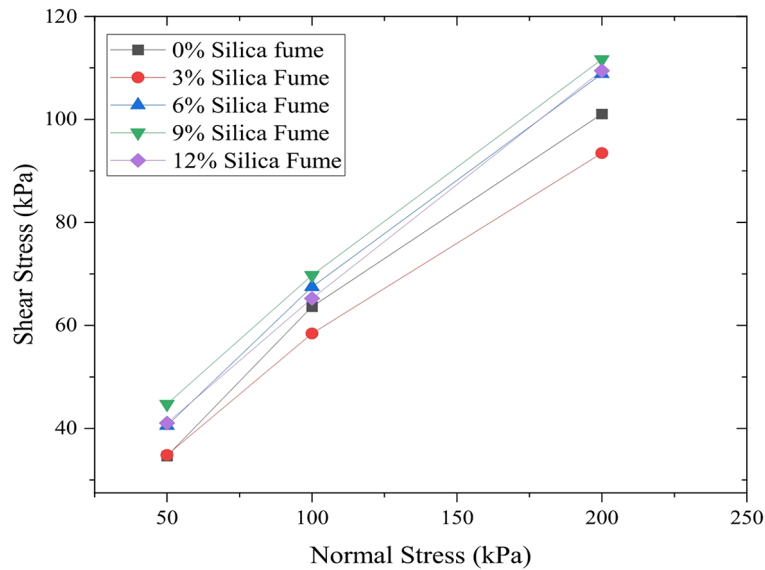


Fig. 14. Mohr-Coulomb failure envelopes obtained from different additive content of silica fume (SF) soil mixtures.

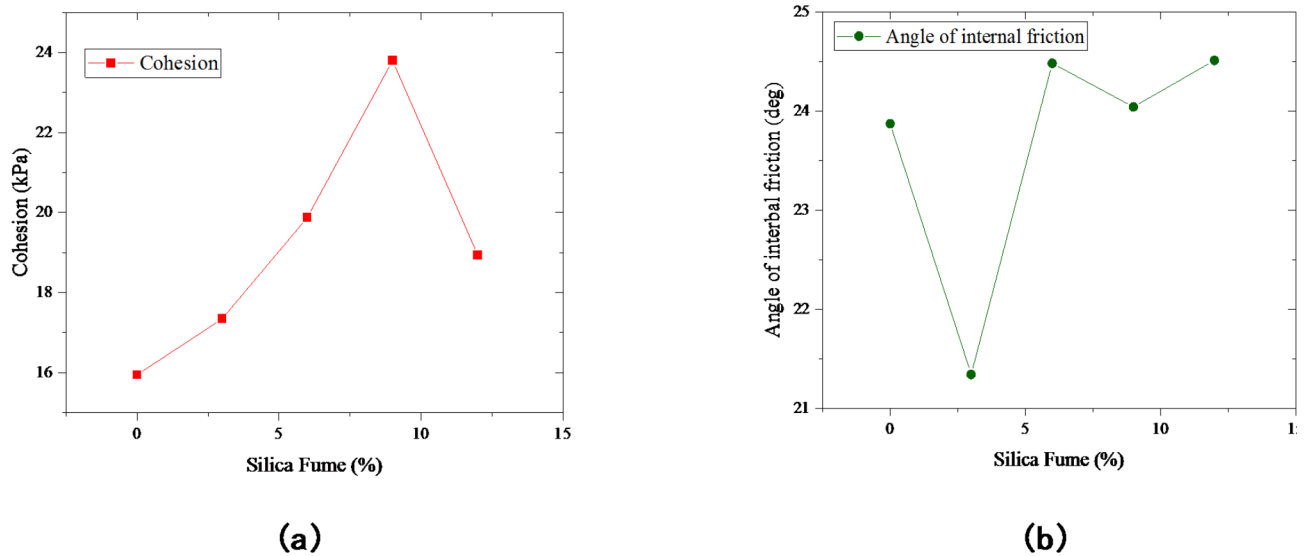


Fig. 15. Variations in shear strength parameters with silica fume (SF) content in soil mixtures: (a) Cohesion (c); (b) Angle of internal friction (ϕ).

process goes on, strengthening the soil matrix even more. Further consolidation results from moisture loss during curing, which also raises the soil's UCS and increases its resistance to deformation.

Direct shear test

Effect of silica fume on cohesion and angle of internal friction on Tarnol soil

Figure 14 illustrates the Mohr-Coulomb failure envelopes for soil mixtures containing silica fume (SF), with normal loads of 50, 100, and 200 kPa applied during the direct shear test. The relationships between silica fume dosage and the angle of cohesion, as well as angle of internal friction, are depicted in Fig. 15(a) and 15(b), respectively. Silica fume was added to the soil samples in varying amounts of 3%, 6%, 9%, and 12%. The maximum shear strength of 111.65 kPa was achieved with a 9% replacement of natural soil with SF. Beyond this threshold, a decline in shear strength was observed. The internal friction angle increased to 24.51°, while cohesion rose from 15.89 kPa to 23.80 kPa. The incorporation of silica fume significantly enhances soil shear strength, with cohesion values increasing by up to 1.49 times and the internal friction angle increasing by up to 1.02 times. Due to pozzolanic interactions between silica fume and calcium hydroxide in the soil, cementitious compounds such as calcium silicate hydrate (C-S-H) are formed, which increases cohesiveness by up to 9%.

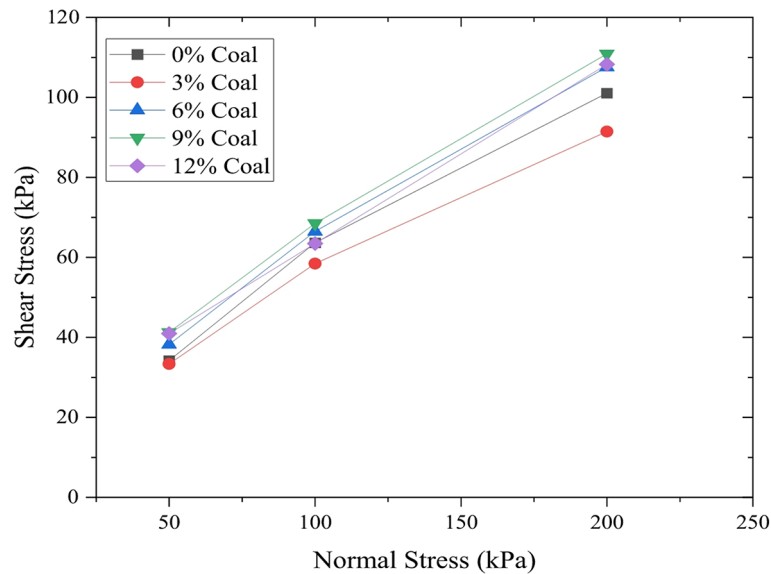


Fig. 16. Mohr-Coulomb failure envelopes obtained from different additive content of coal (C) soil mixtures.

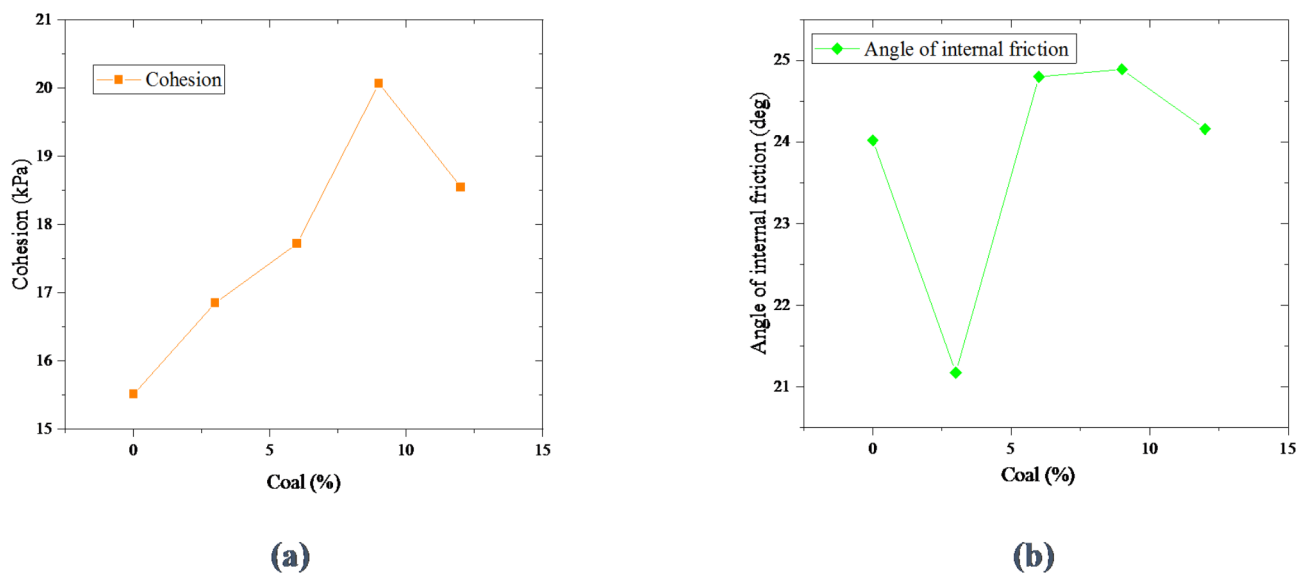


Fig. 17. Variations in shear strength parameters with coal content in soil mixtures: (a) Cohesion (c); (b) Angle of internal friction (ϕ).

However, adding more silica fume does not considerably promote further bonding above 9%. This is due to the fact that when the optimal response between silica fume and soil is achieved, too much silica fume may begin to hinder the compaction and packing of soil particles, hence decreasing cohesiveness⁵².

Effect of coal on cohesion and angle of internal friction on Chaklala soil

Shear strength properties of soil, including cohesion (c) and the internal friction angle (ϕ), were assessed using the direct shear test method. Soil specimens were treated with varying concentrations of coal: 3%, 6%, 9%, and 12%. Direct shear tests were performed under normal loads of 50, 100, and 200 kPa, as shown in Fig. 16. The results indicate that, prior to the addition of coal, the cohesion of the soil was 15.51 kPa. As depicted in Fig. 17(a), the maximum cohesion value of 20.075 kPa was achieved with a 9% coal concentration. Figure 17(b) demonstrates that the maximum internal friction angle, at 24.89°, was also observed with the 9% coal concentration. The highest shear strength parameter, recorded at 110.85 kPa, was observed in the soil mixture containing 9% coal waste. Cohesion increased with coal proportions from 3 to 9% but began to decline at a 12% coal concentration. Increase in cohesion upto 9% coal is because its reactive components encourage pozzolanic reactions with the soil, resulting in the development of cementitious compounds that improve particle bonding. Furthermore, the

filling of soil spaces by coal waste improves compaction. Cohesion, however, decreases after 9% because too much coal waste tends to function as an inert filler, blocking ideal particle packing and decreasing the bonding agents' efficacy. Similarly, the internal friction angle values initially increased from 0 to 3% coal content, peaked at 9%, and then decreased at 12% coal content. The increase in shear strength is attributed to the enhanced mechanical properties of the soil due to the addition of coal waste. Coal waste improves particle binding and packing, resulting in a denser, more stable soil structure that is better able to resist shear forces²⁶. These mechanisms contribute to increased cohesion and the internal friction angle of the soil, thereby enhancing its overall shear strength. Additionally, the porous structure of coal waste, when incorporated into the soil, increases its overall porosity. This increase in void spaces can lead to a better distribution of shear stresses and improved resistance to shear failure. Given the observed enhancements in both cohesion and the internal friction angle, it is rational to conclude that the shear strength of the treated soil is substantially improved. These findings are consistent with prior research studies³⁹.

Effect of silica fume and coal on microstructure analysis

To investigate the microstructural changes in the soil, SEM analyses were carried out on the natural soil samples and an additive content of 12% silica fume (SF). The images from the investigations of the natural soil (Fig. 18a) and the soil sample with a 12% SF additive concentration (Fig. 18b) are shown in Fig. 18. Figure 18a depicts a more dense and dispersed structure in the natural sample. In the case of 12% SF content, it exhibits a more aggregated structure (Fig. 18b). The addition of silica fume (SF) triggers a reaction with calcium hydroxide in the presence of water, leading to the formation of additional cementitious compounds, as shown in Fig. 18. These additional compounds lead to the arrangement of soil particles, transforming from a dispersed structure to a flocculated structure. Additionally, this reaction results in a denser and stronger soil matrix, thereby enhancing its overall strength. SEM analysis reveals that specimens containing 12% SF exhibit a denser and more compact morphology compared to those with 0% SF, as illustrated in Fig. 18. This improvement is attributed to the high dosage of SF, which, at 12%, acts as a filler and exhibits significant pozzolanic effects, thus enhancing the soil's compressive strength. The incorporation of silica fume facilitates the formation of calcium silicate hydrate (CSH) gel, further contributing to the soil's improved structural integrity and calcium hydroxide, making the composite matrix more compact by reducing the soil voids. On the other hand, silica fume, being fine and highly reactive, tends to fill the voids between soil particles, creating a denser and more uniform structure⁵⁹.

Figure 19 displays the images from the investigations of the natural soil (Fig. 19a) and the soil sample with a 12% SF addition concentration (Fig. 19b). A denser and more dispersed structure in the natural sample is shown in Fig. 19a. It displays a more aggregated form when the SF content is 12% (Fig. 19b). Figure 19 illustrates a marked transformation in the soil's structure compared to untreated soil. Coal with reactive components undergoes pozzolanic reactions with soil minerals, leading to the formation of CSH gel compounds that bind soil particles together, enhancing soil stability⁴⁰. The denser and more compact morphology indicates that coal acts as a filler and contributes to the formation of cementitious compounds. As coal interacts with soil particles, it fills voids and enhances binding properties, resulting in a more robust soil matrix. Specimens containing 12% coal demonstrate a denser and more compact structure compared to those without coal, as shown in Fig. 19. Coal particles may coat the surface of soil particles, altering their interaction with water and other particles,

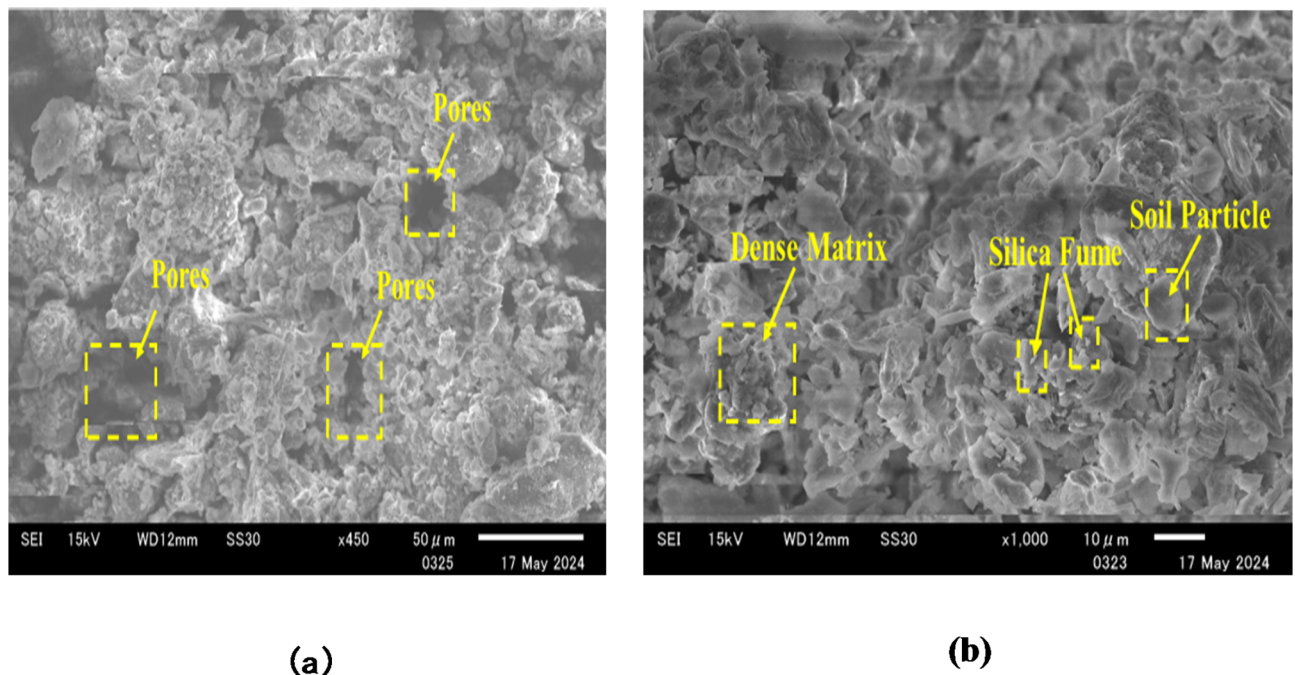
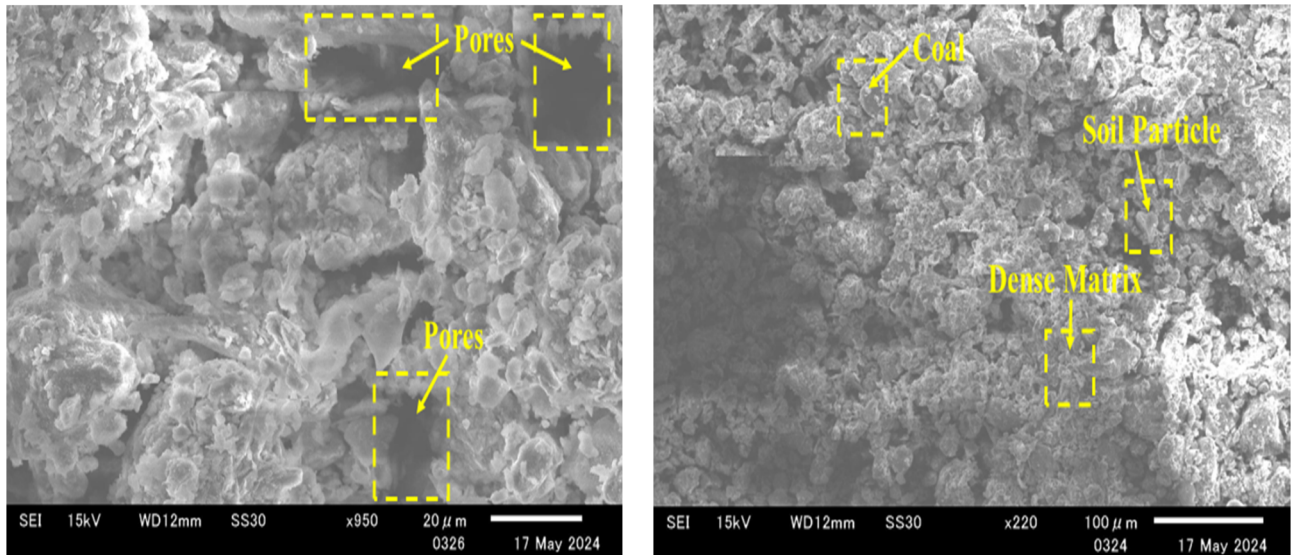


Fig. 18. SEM analysis of: (a) untreated sample; (b) treated sample with 12% SF.



(a) **(b)**
Fig. 19. SEM analysis of: **(a)** untreated sample; **(b)** treated sample with 12% coal.

Parameters	Correlation equation	Variation (%)	R ²
Liquid Limit (LL)	LL = 0.0296SF ² + 0.3505SF + 20.774	96.06	0.9606
	LL = 0.036C ³ - 0.6507C ² + 3.3265 C + 17.449	95.43%	0.9543
Plastic Limit (PL)	PL = 0.0546SF ³ - 0.9497SF ² + 4.1729SF + 17.853	58.21	0.5821
	PL = -0.0298C ⁴ + 0.7058C ³ - 5.0393C ² + 10.569 C + 15	100.00%	1.0000
Plastic Index (PI)	PI = -0.0601SF ³ + 1.0517SF ² - 3.9577SF + 3.2642	69.84	0.6984
	PI = 0.0217C ⁴ - 0.4827C ³ + 3.0835C ² - 4.5304 C + 2.2915	100.00%	1.0000
Unconfined Compressive Strength (UCS) (7 days)	UCS = 9.328SF + 46.828	73.87	0.7387
	UCS = 5.69 C + 42.17	84.37	0.8437
Unconfined Compressive Strength (14 days)	UCS = 9.938SF + 51.028	62.99	0.6299
	UCS = 8.49 C + 42.63	90.08	0.9008
Unconfined Compressive Strength (21 days)	UCS = 11.533SF + 52.703	60.90	0.609
	UCS = 8.65 C + 43.11	88.38	0.8838
Unconfined Compressive Strength (28 days)	UCS = 13.118SF + 54.598	58.86	0.5886
	UCS = 8.74 C + 43.14	88.17	0.8817
Cohesion (c)	c = -0.0883SF ² + 1.4743SF + 15.108	68.11	0.6811
	c = 0.31 C + 15.88	72.98	0.7298
Internal Frictional angle (φ)	φ = -0.0147SF ³ + 0.2837SF ² - 1.2349SF + 23.674	61.28	0.6128
	φ = -0.0208C ³ + 0.3778C ² - 1.5261 C + 23.854	75.48	0.7548

Table 5. Models development through correlation analysis. c = cohesion, φ = internal frictional angle, C = Coal, SF = silica fume, R² = coefficient of determination.

which can reduce the soil's water absorption and improve its stability. Coal waste, when mixed with soil, may show alterations in the soil's particle surface, such as roughness or changes in the bonding between particles. The improved soil structure is evidenced by the tightly packed particles and reduced porosity, which leads to increased compressive strength and overall stability of the soil⁶².

Models development through correlation analysis

Table 5 shows the relationships between various soil parameters and the addition of silica fume (SF) and coal (C) as soil stabilizers. The following models predict over half of the variance in the response variable as the R² (coefficient of determination) value is more than 0.5, indicating a moderate to significant relationship between the prediction and response variables. Over 50% of the variation in the variable that is dependent can be explained

through the independent variables, indicating that this model has a good level of predictive power. Some models in PL and PI are considered highly effective as they predict outcomes based on the provided predictors, with coefficients closer to 1 indicating a greater connection between both independent and dependent variables. An R^2 above 0.5 also suggests that the model fits the data well enough to be useful for making predictions or understanding the relationship between variables. So, this suggests that the models can effectively predict soil parameters when any silica and coal waste content is input into the model. This level of fit is often considered acceptable in many fields, depending on the context and the complexity of the data.

Conclusions

The conclusion summarizes the study's key findings, highlighting the influence of silica fume (SF) and coal (C) on improving the geotechnical properties of low-plasticity soils. Specifically, the addition of SF and coal significantly increased the liquid limit (LL), reduced the plasticity index (PI), and improved shear strength parameters, unconfined compressive strength (UCS), and cohesion of the soils. From the conducted experiments, the following conclusions have been drawn:

- The addition of silica fume (SF) increased the liquid limit (LL) of Tarnol soil by 36% and raised its plastic limit (PL), while the plasticity index (PI) decreased. Conversely, the introduction of coal resulted in a 48% increase in the LL of Chaklala soil and a rise in its PL, with a concurrent reduction in the PI.
- Tarnol soil initially had a maximum dry density (MDD) of 25.568 kN/m³ at an optimum moisture content (OMC) of 11.85%. The incorporation of SF decreased the MDD and increased the OMC. Chaklala soil achieved a maximum dry density of 18.41 kN/m³ at an OMC of 13.53%. The addition of coal also resulted in a decrease in MDD and an increase in OMC.
- For Tarnol soil, the UCS increased from 60.96 kPa to 108.1 kPa after curing, with significant enhancement occurring within the 14-day curing period. For Chaklala soil, UCS rose from 45.5 kPa to 83.2 kPa after 28 days of curing, with the most substantial improvement observed within 14 days.
- Chaklala soil showed an increase in cohesion from 15.51 kPa to 20.075 kPa and in the maximum angle of internal friction from 24.02° to 24.89° with the addition of coal. Specifically, cohesion increased by a factor of 1.29, and the angle of internal friction increased by a factor of 1.04. Similarly, for Tarnol soil, cohesion rose from 15.89 kPa to 23.80 kPa, and the angle of internal friction increased from 23.87° to 24.5°. The incorporation of SF significantly enhanced shear strength, with cohesion values increasing by up to 1.49 times and the internal friction angle values increasing by up to 1.02 times.
- Correlation analysis shows that an R^2 value greater than 0.5 indicates a good correlation between dependent and independent variables. This suggests that the models can effectively predict soil parameters when any silica and coal content is input into the model.

Data availability

Data will be made available on reasonable request from the corresponding author.

Received: 5 August 2024; Accepted: 12 March 2025

Published online: 22 March 2025

References

1. Murthy, V. *Geotechnical Engineering: Principles and Practices of Soil Mechanics and Foundation Engineering* (CRC, 2002).
2. Khalid, B. & Alshawmar, F. J. S. *Exploring the Feasibility of Using Recycled PET Strips with Palm Leaf Ash for Sustainable Soil Stabilization*. Vol. 15(18).13542 (2023).
3. Khalid, B. & Alshawmar, F. J. P. *Comprehensive Review of Geotechnical Engineering Properties of Recycled Polyethylene Terephthalate Fibers and Strips for Soil Stabilization*. Vol. 16(13). 1764 (2024).
4. Yabaluie Khamesluei, M. R., Bayat, M., Mousivand, M. & Nozari, M. A. J. G. Effect of zeolite replacement and tyre fibre inclusions on geotechnical properties of cement-or lime-stabilised sand. *Geoengineering* 1–16 (2024).
5. Rezaei-Hosseinabadi, M. J., Bayat, M. & Nadi, B. Sustainable utilisation of steel slag as granular column for ground improvement in geotechnical projects. *Case Stud. Construct. Mater.* 17, e01333 (2022).
6. Bian, X., Zeng, L., Ji, F., Xie, M. & Hong, Z. Plasticity role in strength behavior of cement-phosphogypsum stabilized soils. *J. Rock Mech. Geotech. Eng.* 14 (6), 1977–1988 (2022).
7. Bian, X. et al. Effects of Biochar on the compressibility of soil with high water content. *J. Clean. Prod.* 434, 140032 (2024).
8. Bian, X., Zeng, L. L., Li, X. Z. & Hong, J. T. Deformation modulus of reconstituted and naturally sedimented clays. *Eng. Geol.* 295, 106450 (2021).
9. Jamil, M. A. B., Hayano, K., Kassa, A., Sekine, R. & Mochizuki, Y. Curing effects on geotechnical properties of clays treated with palm kernel shell Ash and rice husk Ash: insights from water absorption characteristics of stabilizers. *Case Stud. Constr. Mater.* 20, e02947 (2024).
10. Jamil, M. A. B., Hayano, K., Mochizuki, Y. & Li, C. Consolidation characteristics of compacted clayey soils treated with various biomass ashes. *Results Eng.* 24, 103480 (2024).
11. Waleed, M., Liaqat, N., Jamil, M. A. B., Khalid, R. A. & Jamil, S. M. Unconfined compressive strength and freeze-thaw behavior of silty clay soils treated with bio-enzyme. *Arab. J. Geosci.* 16 (4), 275 (2023).
12. Moreno-Maroto, J. M. & Alonso-Azcárate, J. O'Kelly, Review and critical examination of fine-grained soil classification systems based on plasticity. *Soil Classif.* 200, 105955 (2021).
13. Poncelet, N. & François, B. Effect of laboratory compaction mode, density and Suction on the tensile strength of a lime-treated silty soil. *Transp. Geotechnics.* 34, 100763 (2022).
14. Bahari, M., Nikookar, M., Arabani, M., Haghi, A. K. & Khodabandeh, H. Stabilization of silt by nano-clay. In *7th National Congress on Civil Engineering*. 7–8 (2013).
15. Ghani, S., Kumari, S. & Ahmad, S. Prediction of the seismic effect on liquefaction behavior of fine-grained soils using artificial intelligence-based hybridized modeling. *Arab. J. Sci. Eng.* 47 (4), 5411–5441 (2022).
16. Porcino, D. & Diano, V. Laboratory study on pore pressure generation and liquefaction of low-plasticity silty sandy soils during the 2012 earthquake in Italy. *J. Geotech. GeoEnviron. Eng.* 142 (10), 04016048 (2016).

17. Chu, D. B., Stewart, J. P. & Boulanger, R. W. P.-S. Cyclic softening of low-plasticity clay and its effect on seismic foundation performance. *J. Geotechnol. Geoenviron. Eng.* **134**(11), 1595–1608 (2008).
18. Asgari, M. & Baghebanzadeh Dezfuli, A. Experimental study on stabilization of a low plasticity clayey soil with cement/lime. *Arab. J. Geosci.* **8**, 1439–1452 (2015).
19. Turkane, S. D., K. J., S. & Chouksey, M. T. P. Design of low volume road pavement of stabilized low plastic soil using fly Ash geopolymer. *Mater. Today Proc.* **65**, pp. 1154–1160, (2022).
20. Muntohar, A. S., Widiyanti, A. & Hartono, E. Engineering properties of silty soil stabilized with lime and rice husk ash and reinforced with waste plastic fiber. *J. Mater. Civ. Eng.* **25**(9), 1260–1270 (2013).
21. Zhao, X. et al. Feasibility and challenges of multi-source coal-based solid waste (CSW) for underground backfilling – A case study. *Process Saf. Environ. Prot.* **181**, 8–25 (2024).
22. Seco, A., Ramírez, F., Miqueleiz, L. & García, B. Stabilization of expansive soils for use in construction. *Appl. Clay Sci.* **51** (3), 348–352 (2011).
23. Frías, M., De Rojas, M. S., García, R., Valdés, A. J. & Medina, C. Effect of activated coal mining wastes on the properties of blended cement. *Cem. Concr. Compos.* **34** (5), 678–683 (2012).
24. Fauzi, A., Rahman, W. M. N. W. A. & Jauhari, Z. Utilization waste material as stabilizer on Kuantan clayey soil stabilization. *Procedia Eng.* **53**, 42–47 (2013).
25. Li, L., Lei, Y. & Pan, D. Economic and environmental evaluation of coal production in China and policy implications. *Nat. Hazards.* **77**, 1125–1141 (2015).
26. Afrakoti, M. T. P., Choobasti, A. J., Ghadakpour, M. & Kutanaei, S. S. Investigation of the effect of the coal wastes on the mechanical properties of the cement-treated sandy soil. *Constr. Build. Mater.* **239**, 117848 (2020).
27. Modarres, A., Hesami, S., Soltaninejad, M. & Madani, H. Application of coal waste in sustainable roller compacted concrete pavement-environmental and technical assessment. *Int. J. Pavement Eng.* **19** (8), 748–761 (2018).
28. Kavalov, B. & Peteves, S. D. *The Future of Coal* (DG JRC Institute for Energy, European Commission, Petten, 2007).
29. Rahman, M., Pudasainee, D. & Gupta, R. Review on chemical upgrading of coal: Production processes, potential applications and recent developments. *Fuel Process. Technol.* **158**, 35–56 (2017).
30. Stigliani, W.M. Stigliani and assessment, changes in valued capacities of soils and sediments as indicators of nonlinear and time-delayed environmental effects. *Environ. Monit. Assess.* **10**, 245–307 (1988).
31. Al-Mahbashi, A. M., Elkady, T. Y. & Alrefeai, T. O. Soil water characteristic curve and improvement in lime treated expansive soil. *Geomech. Eng.* **8** (5), 687–706 (2015).
32. Aziz, M., Saleem, M. & Irfan, M. Engineering behaviour of expansive soils treated with rice husk Ash [J]. *Geomech. Eng.* **8** (2), 173–186. <https://doi.org/10.12989/gae.2015.8.2.173> (2015).
33. Canakci, H., Aziz, A. & Celik, F. Soil stabilization of clay with lignin, rice husk powder and Ash. *Geomech. Eng.* **8** (1), 67–79. <https://doi.org/10.12989/gae.2015.8.1.067> (2015).
34. Kalkan, E. Impact of wetting–drying cycles on swelling behavior of clayey soils modified by silica fume. *Appl. Clay Sci.* **52** (4), 345–352. <https://doi.org/10.1016/j.clay.2011.03.014> (2011).
35. Kalkan, E. Effects of silica fume on the geotechnical properties of fine-grained soils exposed to freeze and thaw. *Cold Reg. Sci. Technol.* **58** (3), 130–135. <https://doi.org/10.1016/j.coldregions.2009.03.011> (2009).
36. Prabakar, J. & Sridhar, R. Effect of random inclusion of Sisal fibre on strength behaviour of soil. *Constr. Build. Mater.* **16** (2), 123–131. [https://doi.org/10.1016/S0950-0618\(02\)00008-9](https://doi.org/10.1016/S0950-0618(02)00008-9) (2002).
37. Saride, S., Puppala, A. J. & Chikyala, S. R. Swell-shrink and strength behaviors of lime and cement stabilized expansive organic clays. *Appl. Clay Sci.* **85**, 39–45 (2013).
38. Waleed, M., Alshawmar, F., Jamil, M. A. B. & Jafri, T. H. Assessing the stabilization impact of silica fume and phosphogypsum on hydro-mechanical characteristics of clayey sand. *Arab. J. Geosci.* **17** (11), 301. <https://doi.org/10.1007/s12517-024-12108-x> (2024). /10/18 2024.
39. Mansouri, S., Nasiri, M. & Modarres, A. Technical and environmental impacts of coal waste used as a soil stabilizer in construction projects of forest roads. *Croatian J. For. Engineering: J. Theory Application Forestry Eng.* **42** (3), 491–500 (2021).
40. Modarres, A. & Nosoudy, Y. M. Clay stabilization using coal waste and lime—Technical and environmental impacts. *Appl. Clay Sci.* **116**, 281–288. <https://doi.org/10.1016/j.clay.2015.03.026> (2015).
41. Modarres, A. & Nosoudy, Y. M. Clay stabilization using coal waste and lime—Technical and environmental impacts. *Appl. Clay Sci.* **116**, 281–288 (2015).
42. Türköz, M., Umu, S. U. & Öztürk, O. Effect of silica fume as a waste material for sustainable environment on the stabilization and dynamic behavior of dispersive soil. *Sustainability* **13**(8), 4321 (2021).
43. Al-Obaidi, A. A., Al-Mukhtar, M. T. & Al-Dikhil, O. M. Comparative study between silica fume and nano silica fume in improving the shear strength and collapsibility of highly gypseous soil. *Tikrit J. Eng. Sci.* **27**(1), 72–78 (2020).
44. AL-Soudany, K. Y. Improvement of expansive soil by using silica fume. *Kufa J. Eng.* **9** (1), 222–239 (2018).
45. Harris, D., Heidrich, C. & Feuerborn, J. *Global Aspects on Coal Combustion Products* (2019).
46. Tumuluru, J. S., Wright, C. T., Boardman, R. D., Yancey, N. A. & Sokhansanj, S. A review on biomass classification and composition, co-firing issues and pretreatment methods. In *2011 Louisville, Kentucky, August 7–10*. Vol. 1 (2011).
47. Rahman, M. A. & Ahmed, A. Use of silica fume in stabilizing cement-dune sand for highway materials. *Am. J. Civ. Eng.* **51**, 41–49 (2017).
48. Barbhuiya, S. & Qureshi, M. Effects of silica fume on the strength and durability properties of concrete, *Age* **3**(7), 28 (2016).
49. Sharaky, I., Megahed, F., Seleem, M. & Badawy, A. The influence of silica fume, nano silica and mixing method on the strength and durability of concrete. *SN Appl. Sci.* **1**, 1–10 (2019).
50. Atiş, C. et al. Influence of dry and wet curing conditions on compressive strength of silica fume concrete. *Build. Environ.* **40** (12), 1678–1683 (2005).
51. Kalkan, E. & Akbulut, S. The positive effects of silica fume on the permeability, swelling pressure and compressive strength of natural clay liners. *Eng. Geol.* **73**(1–2), 145–156 (2004).
52. Rapulane, K. S. *Modified Silica Fume Soil Stabilisation of Marginal-Road Subgrades* (University of Johannesburg (South Africa), 2021).
53. D. ASTM, 2166. *Standard test method for unconfined compressive strength of cohesive soil* (West Conshohocken, 2016).
54. D.-. ASTM. *Standard test method for direct shear test of soils under consolidated drained conditions*. D3080/D3080M. Vol. 3(9) (2011).
55. Fattah, M. A. et al. Characteristics of clays stabilized with lime-silica fume mix. *Ital. J. Geosci.* 104–113 (2015).
56. Al-Azzawi, A. D. & Sattar, A. *Khalida Effect of Silica Fume Addition on the Behavior of Silty-Clayey Soils*.
57. Turan, C. J. et al. Geotechnical characteristics of fine-grained soils stabilized with fly ash, a review. *Sustainability* (2022).
58. Seyrek, E. Engineering behavior of clay soils stabilized with class C and class F fly ashes. *Sci. Eng. Compos. Mater.* **25** (2), 273–287 (2018).
59. Tiwari, N., Satyam, N. & Singh, K. Effect of curing on micro-physical performance of polypropylene fiber reinforced and silica fume stabilized expansive soil under freezing thawing cycles. *Sci. Rep.* **10** (1), 7624 (2020).
60. Al-Azzawi, A. A., Daud, K. A. & Sattar, M. A. A. Effect of silica fume addition on the behavior of silty-clayey soils. *J. Eng. Sustainable Dev.* **16** (1), 92–105 (2012).

61. Al-Obaidi, A. A., Al-Mukhtar, M. T., Al-Dikhil, O. M. & Hannona, S. Q. Comparative study between silica fume and nano silica fume in improving the shear strength and collapsibility of highly gypseous soil. *Tikrit J. Eng. Sci.* **27** (1), 72–78 (2020).
62. Ziari, H., Zalnezhad, M., Ziari, M. A., Amiri, E. N. Substitution of the natural aggregate filler by coal waste powder (CWP) in microsurfacing surface treatment: Mix design and performance evaluation. *Road Mater. Pavem. Des.* **354**, 129132 (2022).

Acknowledgements

The Researchers would like to thank the Deanship of Graduate Studies and Scientific Research at Qassim University for financial support (QU-APC-2025).

Author contributions

Muhammad Waleed and Fahad Alshawmar contributed equally to this work.

Declarations

Competing interests

The authors declare no competing interests.

Additional information

Correspondence and requests for materials should be addressed to F.A.

Reprints and permissions information is available at www.nature.com/reprints.

Publisher's note Springer Nature remains neutral with regard to jurisdictional claims in published maps and institutional affiliations.

Open Access This article is licensed under a Creative Commons Attribution-NonCommercial-NoDerivatives 4.0 International License, which permits any non-commercial use, sharing, distribution and reproduction in any medium or format, as long as you give appropriate credit to the original author(s) and the source, provide a link to the Creative Commons licence, and indicate if you modified the licensed material. You do not have permission under this licence to share adapted material derived from this article or parts of it. The images or other third party material in this article are included in the article's Creative Commons licence, unless indicated otherwise in a credit line to the material. If material is not included in the article's Creative Commons licence and your intended use is not permitted by statutory regulation or exceeds the permitted use, you will need to obtain permission directly from the copyright holder. To view a copy of this licence, visit <http://creativecommons.org/licenses/by-nc-nd/4.0/>.

© The Author(s) 2025